IEEE Access
Multidisciplinary | Rapid Review | Open Access Journal

Received 29 May 2024, accepted 20 June 2024, date of publication 26 June 2024, date of current version 5 July 2024.

Digital Object Identifier 10.1109/ACCESS.2024.3419553

APPLIED RESEARCH

2.4 GHz Fully Woven Textile-Integrated Circularly Polarized Rectenna for Wireless Power Transfer Applications

MIGUEL FERNÁNDEZ, CARLOS VÁZQUEZ, AND SAMUEL VER HOEYE, (Member, IEEE)
Electrical Engineering Department, University of Oviedo, 33203 Gijón, Spain

Corresponding author: Miguel Fernández (fernandezgmiguel@uniovi.es)

This work was supported in part by the Ministerio de Ciencia e Innovación-Gobierno de España under Project PID2021-126301NA-I00 and Project EQC2019-005768-P; in part by the Gobierno del Principado de Asturias under Project AYUD/2021/51706, Project IDI/2021/000207, Project IDI/2020/000220, and Project IDI/2018/000191; and in part by Universidad de Oviedo under Project GR-2010-0015.

ABSTRACT In this work, a 2.4 GHz fully woven textile-integrated circularly polarized rectenna intended for wireless power transfer applications is presented. A rectangular patch with truncated corners is used as the radiating element. It is fed through a T-match structure, which allows the control of the input impedance without requiring any additional impedance-matching network. A single-diode rectifier topology was considered to simplify the entire structure and to facilitate its integration with the antenna. The rectifier and the antenna are optimized together through a co-simulation strategy, in which the input impedance of the antenna is adjusted to match the input impedance of the rectifier, ensuring maximum power transfer between them. At the implementation stage, the rectifier is first mounted on a carrier thread, which is then incorporated into the woven structure. This approach, in combination with the chosen antenna feeding technique, which requires no additional elements for impedance matching purposes, provides a high degree of integration between the antenna and the rectifier. The rectenna was experimentally characterized, providing a 45% overall efficiency under realistic working conditions.

INDEX TERMS Antennas, rectenna, rectifier, textile technology, wireless power transfer.

I. INTRODUCTION

The development of the Internet of Things (IoT) technology has experienced rapid growth, boosting the demand for wireless sensors. Among the large number of potential applications, textile devices capable of being integrated into fabrics are attractive in the fields of healthcare and sports, because they allow the implementation of wearable sensors to monitor vital signs, while causing minimal disturbance to the user.

The DC power supply of the sensors remains a challenge in the development of wearable devices. The use of batteries increases the size, weight, and cost of the devices. In addition, the necessity of periodic recharges and/or battery substitution has a negative impact on the user experience. Energy Harvesting (EH) and Wireless Power Transfer (WPT) approaches have been proposed to avoid the use of batteries and are nowadays being considered as enabling technologies for the development of sensor networks [1]. In the case of the EH approach, the device converts the RF energy available in the environment from non-dedicated sources, such as radio or TV transmitter stations, mobile phone base stations, or Wi-Fi access points [2], [3], [4], into DC energy. Because the RF sources are non-dedicated, and the RF energy available to be harvested strongly depends on the location, EH devices must be designed to collect energy from different source systems working in different frequency bands [3]. Thus, in general, they are required to simultaneously exhibit multiband and broadband characteristics, which complicates the impedance matching between the antenna and the rectifier, with a

The associate editor coordinating the review of this manuscript and approving it for publication was Zahra Shaterian.

negative impact on the overall performance. On the other hand, the WPT approach is based on the use of a dedicated RF transmitter. Hence, a higher and more predictable DC power level is generally obtained [5]. Furthermore, the use of a narrowband dedicated RF source simplifies the impedance matching between the antenna and the rectifier, providing considerably higher efficiency values.

The research effort carried out in the last few years has provided a number of works describing techniques [6], [7] to design rectennas [7] and arrays [8] on rigid substrates, reporting state-of-the-art efficiency values around 70% when the rectifier input power is about 0 dBm, at 2.4 GHz. In the case of textile devices, several implementation techniques with different integration levels between the antenna and the rectifier, and between the rectenna and the fabric, have been reported. In [9], a rectenna implemented on a flexible substrate and concealed in a fabric pocket is described, providing the most basic degree of integration. A different textile implementation strategy consists in stacking shaped conductive and dielectric fabric layers, attaching them with adhesive. This technique was applied in [10], [11], and [12] to obtain a dual polarization circular patch, a rectangular and a dual-band rectangular patch antennas, respectively. In [13], a submm-wave band broadband rectenna, in which the radiating surfaces, the ground plane and the rectifier layout are implemented on a flexible nontextile substrate which is then stacked with a felt fabric, which acts as a dielectric. A similar implementation is presented in [14], in which the rectifier and the feeding structure are implemented in a conventional PCB. Textile embroidered rectennas were also presented. In [15], a dual polarization patch antenna, without rectifier is described, whereas [16] presents a patch array rectenna. In addition, a large bow tie array screen-printed on a cotton fabric, was reported in [17]. In all the previous cases, the rectifier layout is implemented using the same technique as for the radiating elements, with the exception of [11] and [14], in which the rectifier is implemented on an external PCB, reaching a moderate degree of integration between the antenna and the rectifier.

A different approach for the implementation of textile RF subsystems and antennas, based on the use of fully-woven structures has also been proposed. This technology has been applied to the design of microwave waveguides [18], frequency selective surfaces [19], [20], and antennas [21], [22]. Furthermore, LF [23] and UHF [24] RFID tags were developed by combining fully-woven structures with external circuitry, providing a high degree of integration while keeping the advantages of woven devices, i.e., robustness, design flexibility depending on the loom technology, ease of integration with larger elements, and the capability of large-scale production using conventional processes from the textile industry.

In this work, the first fully-woven textile rectenna with circular polarization intended for WPT applications in the 2.4 GHz band is presented. The radiating element is based on a rectangular patch with two truncated corners, which provides circular polarization, in order to mitigate potential polarization mismatches between the transmitter antenna and the rectenna. A T-match structure is used as the feeding technique, in order to control the antenna input impedance, maximizing the power transfer between the antenna and the rectifier. Moreover, the complete structure is suitable for fabrication in fully-woven technology. On the other hand, the rectifier is integrated with the antenna using the technique presented in [24]. The rectifier is first mounted on a carrier thread, which can then be handled by the loom at the weaving stage to incorporate it in the woven structure, providing a robust implementation with a maximum degree of integration.

The paper is organized as follows. Section II presents the rectenna overview. The detailed design and optimization of the antenna and the rectifier are covered in Section III. Section IV briefly describes the implementation technique, and the experimental results are presented in section V.

II. RECTENNA OVERVIEW

A. TOPOLOGY

The proposed fully-woven rectenna, including the radiating element and the rectifier circuit, is schematized in Fig. 1. The design of the radiating element is based on a rectangular patch. It combines the use of two chamfered corners with a T-match feeding structure to obtain a compact layout compatible with woven textile technology, while it is able to simultaneously provide circular polarization and complex conjugate impedance matching to the rectifier, without requiring additional matching networks. The T-match network parameters are optimized, together with the patch dimensions, for the antenna input impedance, Z_{ant}, to be close to the complex conjugate of the rectifier input impedance Z^*_{rec}, ensuring maximum power transfer between them. Furthermore, the ground plane, which is an inherent part of the selected radiating structure, provides isolation between the antenna and potential underlying objects, making it suitable for a wide variety of applications and scenarios.

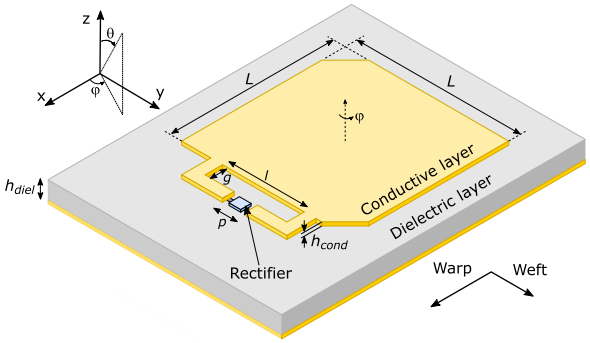

FIGURE 1. Rectenna topology. The rectifier is integrated with a patch antenna fed through a T-match structure. Dimensions (in mm): $L = 40.1$, $l = 8$, $g = 8.6$, $p = 6$, $h_{diel} = 0.8$.

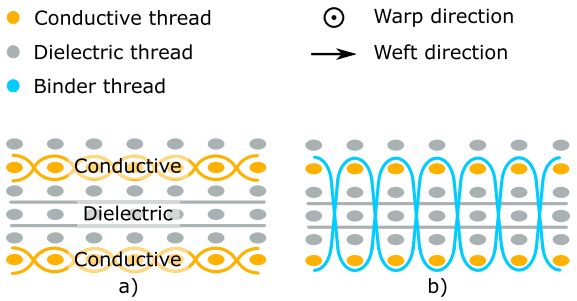

FIGURE 2. Fabric structure. a) Conductive and dielectric thread structure of the multilayer fabric. b) Dielectric binder thread structure.

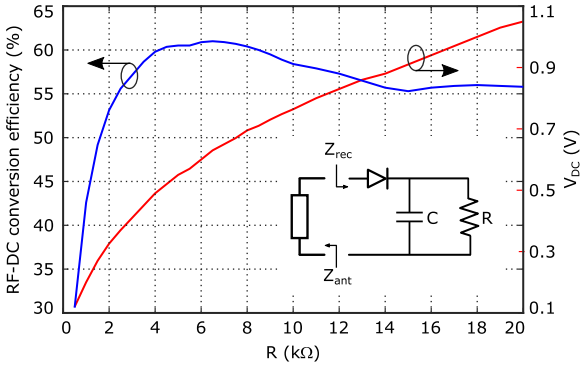

FIGURE 3. Maximum RF-DC conversion efficiency and output voltage V_{DC} vs. the resistor value R. Inset: topology of the rectifier.

On the other hand, a single-diode rectifier is used. It is mounted on a carrier thread and then integrated with the antenna by connecting it to the T-match network terminals, in a similar way as described in [24], which allows a high degree of integration and robustness, since no soldered unions between electronic components and textile pads are required.

B. FULLY-WOVEN STRUCTURE OF THE ANTENNA

The proposed fully-woven textile rectenna is designed on a multilayer fabric intended to be manufactured in a single step, using an industrial loom. The fabric includes two conductive layers separated by a dielectric layer. One of the conductive layers acts as ground plane, whereas the radiating patch layout is structured on the other one.

Since the textile rectenna is intended to be manufactured using an industrial loom, it is composed of warp and weft threads, which are perpendicular to one another. The warp threads are aligned with the length of the fabric and mounted in the loom before starting the manufacturing process. On the other hand, the weft threads are aligned with the width of the fabric and added along the weaving process.

Both the warp and the weft threads can be conductive or dielectric, depending on the layer of the fabric. In this case, the conductive layers are woven with *ELITEX 117/f17 2ply* threads. Each one is formed by two twisted 17 filament yarns. The filaments are made of polyamide with a 1 μm thick silver coating, providing a linear resistance value around 70 Ω/m. On the other hand, the dielectric layer is formed by polyester threads composed of two twisted multifilament yarns.

The thread level structure of the fabric is similar to that described in [24], as schematized in Fig 2. The top and bottom conductive layers are made from woven conductive warp and weft threads. The dielectric section of the fabric is composed of five nonwoven layers of dielectric threads. Finally, dielectric binder threads are used to hold the structure together. Their location in the fabric is schematized in Fig 2 b), in which the warp conductive threads are not represented for the sake of clarity.

Finally, note that all the required conductive and dielectric layers are part of the same woven structure. Thus, the use of the woven technology is expected to provide improved robustness with respect to nonwoven technologies, in which several independent fabric sheets have to be attached together in some way.

III. DESIGN AND OPTIMIZATION

The antenna and the rectifier were optimized using a co-simulation strategy, aimed at maximizing the power transfer between them. First, the rectifier was optimized and its input impedance, Z_{rec}, calculated through the Harmonic Balance (HB) technique implemented in the *Keysight ADS* package. On the other hand, the antenna was modeled and its input impedance, Z_{ant}, calculated through the Finite Element Method (FEM), implemented in *Ansys HFSS*. Note that the goal is to adjust the input impedance of the antenna to achieve $Z_{ant} \approx Z_{rec}^*$.

A. RECTIFIER

The topology of the rectifier is shown in the inset of Fig. 3. It is based on a single *BAT 15-04W* Schottky diode, from Infineon, and two discrete components, resulting in a layout easily integrable with the textile antenna. The value of the capacitor, $C = 1$ nF, was selected to short circuit the 2.4 GHz RF signal at the diode output, and the resistor R represents the load that should be driven by the rectifier, which is application dependent. The output DC voltage, V_{DC}, is taken at the resistor terminals.

Nonlinear simulations based on the HB technique were conducted to calculate the RF-DC conversion efficiency ν and the output DC power P_{DC} and voltage V_{DC}, and to determine the rectifier input impedance Z_{rec} as a function of R. The frequency and available power of the input RF signal are $f_{RF} = 2.4$ GHz and $P_{RF} = -10$ dBm, respectively, and optimum input impedance matching is considered. The P_{DC} and V_{DC} values as a function of R, are represented in Fig. 3. In this work, the resistor value is set to $R = 5.1$ kΩ, to maximize the RF-DC conversion efficiency while providing a DC output voltage $V_{DC} \approx 0.5$ V. Under the described conditions, the input impedance is $Z_{rec} = 15 - j185$ Ω. Thus, the expected RF-DC conversion efficiency will be around 60% when the impedance of the RF signal source, i.e., the antenna port in the whole rectenna,

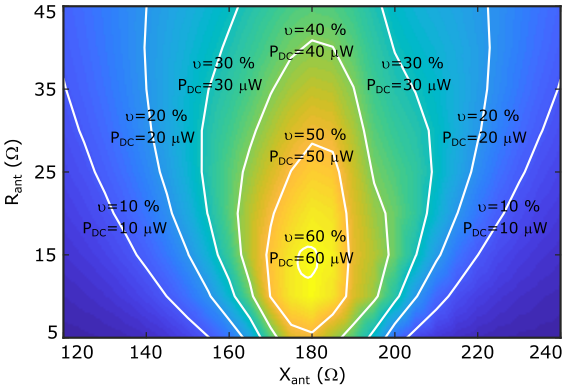

FIGURE 4. RF-DC conversion efficiency ν of the rectifier as a function of the real and the imaginary parts of the generator (antenna) impedance. The corresponding DC output power when $P_{RF} = -10$ dBm is also indicated.

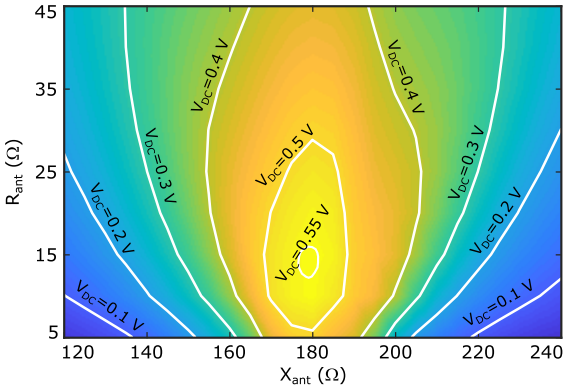

FIGURE 5. Evolution of the output DC voltage with the generator impedance when the input power is $P_{RF} = -10$ dBm.

is $Z_{ant} = Z^*_{rec} = 15 + j185\ \Omega$. Nevertheless, the represented data can be used to select the optimum value of R to meet the requirements of each particular application, i.e., the best trade-off between power conversion efficiency and output DC voltage.

Since it is not realistic to assume that the input impedance of the antenna will exactly match the optimum value, the evolution of the RF-DC conversion efficiency with the impedance of the signal generator (Z_{ant} when the rectifier is integrated as a part of the rectenna) was calculated and represented in Fig. 4, together with the associated output DC power values, provided that the input power is $P_{RF} = -10$ dBm. As can be observed, any value of the real part R_{ant} in the 5-25 Ω range, combined with an imaginary part X_{ant} in the 170-190 Ω range, result in a conversion efficiency higher than 50%, which provides certain degree of flexibility when designing the textile antenna. This is a valuable characteristic, since the dimensional accuracy that can be achieved when implementing the textile antenna is not as high as in the case of conventional PCB technology. In addition, Fig. 5 represents the evolution of V_{DC} with the generator impedance, when the input power is $P_{RF} = -10$ dBm.

B. EM MODELING OF WOVEN STRUCTURES

The high geometrical complexity of woven structures, which can be observed in Fig. 2, makes their electromagnetic modeling a demanding task [24]. Furthermore, each thread is, in general, composed of several filaments. Thus, the accurate modeling of the fabric structure requires a high-density mesh, resulting in a computationally complex problem. To overcome that issue, some strategies were described to reduce the model complexity while preserving its accuracy [26], [27]. In the case of the dielectric layers, they were modeled as a homogeneous sheet with the same thickness h_{diel} as the original layer and with an equivalent dielectric permittivity $\varepsilon_{r,eq}$. This value is reduced with respect to that of polyester, due to the air gaps in the woven structure. The air percentage in the woven structure and, therefore, the value of $\varepsilon_{r,eq}$, depends on the epi and ppi loom parameters, which indicate the number of warp and weft treads per inch, respectively. Furthermore, the air gaps inside each thread made from several filaments also impacts the value of $\varepsilon_{r,eq}$. Here, $\varepsilon_{r,eq}$ was estimated from the experimental characterization of a transmission line and a resonator implemented on a fabric sample, obtaining $\varepsilon_{r,eq} \approx 1.8$, and $\tan\delta \approx 0.04$.

Regarding the conductive layers, the conductive threads used in this work are obtained by silver coating conventional polyester threads. Moreover, when considering the conductive fabric, the current can flow in any direction, because of the very large number of interconnections between warp and weft threads that are formed at the weaving stage. Thus, each conductive layer can be modeled as a homogeneous conductive sheet with thickness $h_{cond} = 1\ \mu$m and conductivity $\sigma_{eq} = 6.3 \times 10^7$ S/m, similar to those of the filament coating.

C. ANTENNA DESIGN AND OPTIMIZATION

The design of the radiating element starts from a square patch whose side length $L = 40.1$ mm is selected to resonate at 2.4 GHz. The patch is fed through a T-match structure which allows a relatively easy control of the antenna input impedance Z_{ant}, and provides the required inductive component to match the capacitive input impedance of the rectifier. Finally, two diagonally opposite corners were chamfered to produce circular polarization. Since this operation modifies the patch size, the length L and the feeding network parameters had to be reoptimized to maintain the desired input impedance at 2.4 GHz.

Once the size of the patch is fixed, a parametric analysis was conducted to determine the dependence of the antenna input impedance Z_{ant} on the T-match network parameters. It was observed that both the real and the positive imaginary parts of Z_{ant} increase with the total length of the loop formed by the T-match network arms and the patch edge, i.e., with larger values of l and/or g. On the other hand, moving the interconnection points between the network and

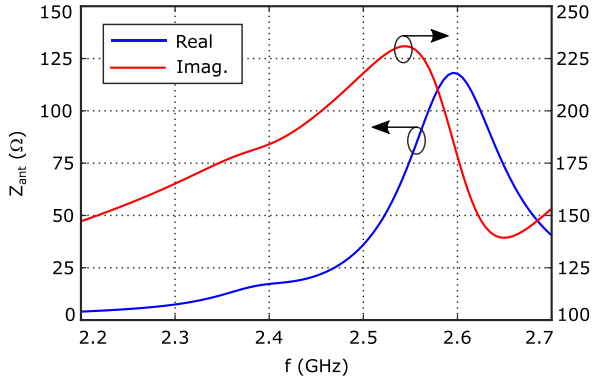

FIGURE 6. Evolution of the antenna input impedance Z_{ant} with frequency.

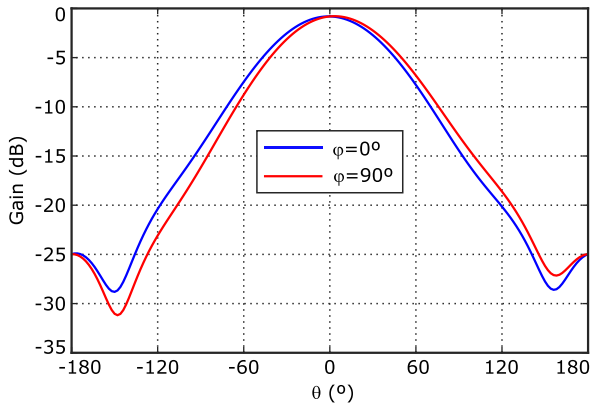

FIGURE 7. Simulated gain evaluated in the main planes $\varphi = 0^o$ and $\varphi = 90^o$, at 2.4 GHz.

the patch edge to the edge center, i.e., reducing the value of g, reduces the real part of Z_{ant}, while the imaginary part remains almost unchanged. The values of the optimized parameters are shown in the caption of Fig. 1. For simplicity, the width of the T-match arms is kept constant at $w = 2$ mm, and the port width is set to $p = 6$ mm, which is large enough to accommodate the rectifier. The chamfered corners are obtained by cutting off the two corresponding adjacent edges 5.5 mm from the initial vertex. The evolution of the input impedance of the optimized antenna with frequency is represented in Fig. 6, resulting in $Z_{ant} = 17 + j185\ \Omega$ at 2.4 GHz, which should provide an RF-DC conversion efficiency around 60%, when used in combination with the rectifier.

The radiation pattern, evaluated in the XZ ($\varphi = 0^o$) and YZ ($\varphi = 90^o$) planes is displayed in Fig. 7. The simulated maximum gain is around -1 dB because of the high tanδ value of the textile substrate. Finally, the axial ratio, evaluated in the main planes at 2.4 GHz, is represented in Fig. 8, showing that the antenna exhibits circular polarization in a $-60 < \theta < 60^o$ angular range. On the other hand, the simulated axial ratio is under 3 dB in the $2.38 - 2.42$ GHz frequency range, whereas the antenna input impedance Z_{ant} varies from $11 + j182\ \Omega$ to $16 + j190\ \Omega$ in that range,

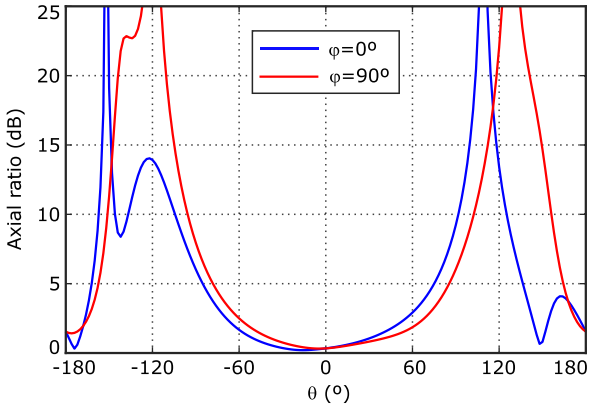

FIGURE 8. Simulated axial ratio evaluated in the main planes $\varphi = 0^o$ and $\varphi = 90^o$, at 2.4 GHz.

which should provide a minimum RF-DC conversion efficiency larger than 50% (see Fig. 4).

IV. IMPLEMENTATION

This section describes the manufacturing processes of the antenna and the rectifier, as well as the integration between them.

A. ANTENNA

The radiating element was implemented starting from a fully-woven fabric composed of an inner dielectric part covered by two conductive layers, as schematized in Fig. 2. The radiating element and the feeding network were structured on the top layer by laser cutting the conductive threads and then manually removing the segments not belonging to the design.

B. RECTIFIER

In order to obtain a high degree of integration with the textile antenna, the rectifier was implemented on a flexible substrate and then mounted on a dielectric carrier thread, in a similar way as described in [24].

First, a polyimide strip was silver coated and patterned to generate the pads for the discrete components (diode, resistor and capacitor), the interconnections between them, and the contact areas with the fabric. Next, the components were mounted and protected with epoxy resin. Finally, a dielectric carrier thread was glued to the back side of the polyimide strip. A picture of the rectifier mounted on the carrier thread is shown in Fig. 9 a), whereas part b) represents the manufactured rectenna.

Since the rectifier is mounted on a carrier thread, it can be handled by the loom as a weft thread, enabling the integration with the textile antenna at the weaving process. Therefore, the silver coated arms of the polyimide strip are woven together with the conductive threads that constitute the antenna feeding structure, generating a large number of contact points which ensure the electrical connection between the antenna and the rectifier. In this way, no soldered

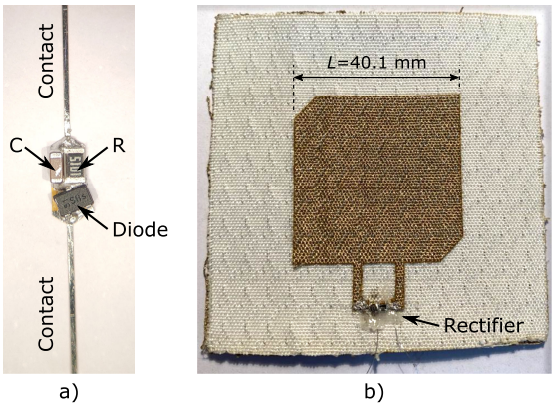

FIGURE 9. a) Rectifier mounted on a carrier thread. b) Manufactured rectenna.

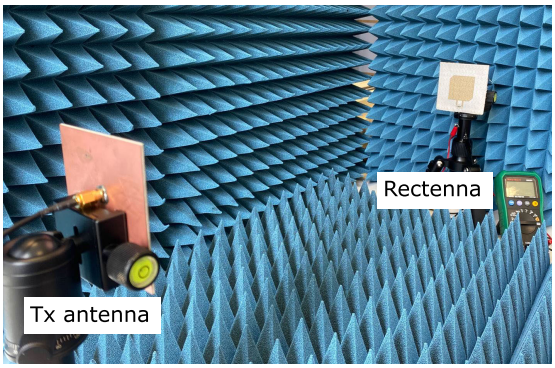

FIGURE 10. Measurement setup. A conventional linearly polarized rectangular patch antenna is used at the transmitter side.

joints with fabric parts are required, increasing the rectenna robustness.

V. EXPERIMENTAL CHARACTERIZATION

A. MEASUREMENT SETUP

The transmitter side of the measurement setup is composed of an RF signal source and a linearly polarized patch antenna working at $f_{RF} = 2.4$ GHz. The transmitter antenna gain is $G_{TX} \approx 5$ dB, and the signal power is set to a maximum of 22 dBm, in order not to exceed the European EIRP limit for transmitters operating at indoor environments. At the receiver side, a multimeter is used to measure the DC voltage V_{DC} generated by the developed rectenna. That DC voltage signal is taken at the resistor terminals, and it can be easily converted into a DC power value P_{DC}, taking into account the resistor value $R = 5.1$ kΩ.

The nominal distance between the transmitter antenna and the rectenna was set to $d = 0.5$ m, for which the free space propagation loss is about 34 dB. Thus, taking into account a 3 dB additional loss due to the fact that the transmitter antenna is linearly polarized, whereas the rectenna exhibits circular polarization, the estimated value of the available RF power at the rectifier input is $P_{RF} \approx -10$ dBm. A picture of the measurement setup is shown in Fig. 10

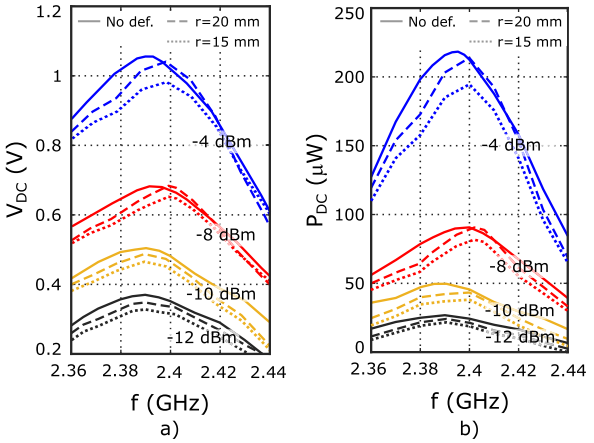

FIGURE 11. a) Evolution of the measured V_{DC} (a) and P_{DC} (b) with the working frequency, for different estimated RF power values available at the rectifier input. Solid line: no deformation. Dashed line: bent rectenna. For the sake of clarity, only the # 1 deformation case schematized in the inset of Fig. 13 has been considered.

B. RESULTS

First, the evolution of the output DC voltage and power with the working frequency was evaluated and represented in Fig. 11. As expected, the best values are achieved around 2.4 GHz because of the optimum performance of the T-match feeding network at that frequency. Nevertheless, the variation with frequency is smooth because relatively large changes on the antenna input impedance cause small variations on the RF-DC conversion efficiency, as indicated in Fig. 4. Furthermore, the performance of the rectenna was also evaluated for other available power values at the rectifier input. The rectenna performance improves as the available power at the rectifier input increases because the Schottky diode is driven further into the on region of the junction. This experimental data can be used to estimate the system behavior when the transmitter is allowed to operate with higher EIRP, or in applications in which the distance between the dedicated transmitter and the rectenna is reduced.

On the other hand, Fig. 12 shows the RF-DC conversion efficiency of the rectifier, referred to the input available power (dashed line), and the rectenna overall efficiency, taking into account the antenna gain (solid line). In the case of the rectifier, the measured efficiency is slightly smaller than the expected from the simulation data, which is probably due to inaccuracies in the diode simulation model. When analyzing the overall efficiency of the rectenna, it is reduced because the gain of the textile antenna is smaller than 0 dB. Furthermore, since the transmitter antenna is linearly polarized, and the rectenna is expected to have circular polarization, it only accepts half of the incident power. Thus, a $\times 2$ correction factor was applied to compute the real conversion efficiency.

Regarding the polarization of the rectenna, it was rotated around the normal direction to the patch plane ($\hat{z}$ in Fig. 1) from $\varphi = 0^o$ to 90^o, in 15^o steps, measuring the generated

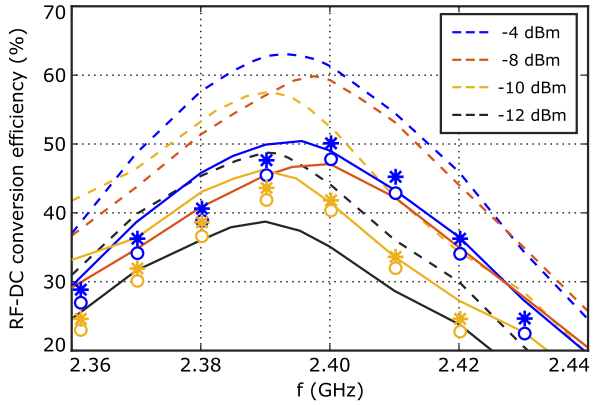

FIGURE 12. RF-DC conversion efficiency calculated from the measured DC voltage. Solid line: overall rectenna efficiency. Dashed line: rectifier efficiency. The '∗' and 'o' points correspond with the rectenna bent with radius $r = 20$ and $r = 15$ mm, respectively. For the sake of clarity, only the # 1 deformation case schematized in the inset of Fig. 13 has been considered.

DC voltage for each position. The resulting rectified DC power, when the working frequency is 2.4 GHz, expressed in dBm is represented in Fig. 13. As can be observed, the measured power variation is smaller than 3 dB, indicating that the antenna exhibits circular polarization.

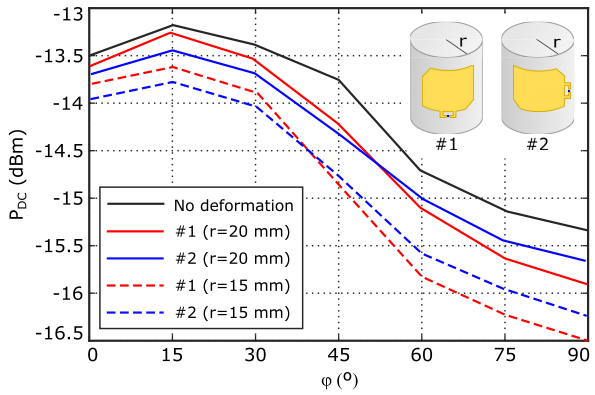

FIGURE 13. Measured DC power when the antenna rotates around its normal axis, under different bending conditions. The working frequency is $f_{RF} = 2.4$ GHz.

The impact of deformations on the rectenna performance was also evaluated. The prototype was deformed to match the surface of a cylinder in the two directions schematized in the inset of Fig. 13, considering two curvature radii: $r = 20$ mm and $r = 15$ mm, and the generated DC voltage and power were evaluated in the same scenarios as previously described. The results are shown in Figs. 11, 12, and 13 together with the measured values without deformation. Although the performance is slightly degraded when deforming the rectenna, mainly due to the fact that, after bending it, the antenna is no longer illuminated by a plane wave, the reduction of the RF-DC conversion efficiency is smaller than 5% and the bent antenna is still circularly polarized.

C. COMPARISON WITH THE STATE-OF-THE ART

Table 1 compares the results from the woven rectenna presented in this work with other textile nonwoven designs reported in the last few years. First, the best performance in terms of RF-DC conversion efficiency, and required available power at the rectifier input, is obtained when working at frequencies below 1 GHz, because of the intrinsic characteristics of Schottky diodes.

TABLE 1. Comparison with the state-of-the-art.

Ref.	Freq. (GHz)	RF-DC conv. eff. (%)	Rect. available power (dBm)	Polarization
[10]	0.82	42	-20	Dual linear
[12]	0.82	62	-	Linear
[9]	1	30	-10	Linear
[11]	2.45	30	-10	Linear
[14]	2.45	56	-5	Circular
[16]	2.45	35	-10	Linear
This work	2.4	45	-10	Circular

Focusing on the 2.4 GHz band, this work provides a conversion efficiency value comparable with the maximum reported [14], but the required available power at the rectifier input in [14] is −5 dBm, which is only achievable in an unrealistic scenario from the point of view of the transmitted power and/or the distance between the transmitter and the rectenna. Note that most of the works provide the required available power at the rectifier input, thus measuring the efficiency of the rectifier, instead of the overall value. In this case, the measured DC-RF conversion efficiency of the rectifier is about 55% when the available input power is −10 dBm, whereas the overall rectenna efficiency is 45% in the same scenario.

Finally, most of the works report nonwoven textile antennas. With the exception of [9], in which a wire antenna and the rectifier are implemented in conventional flexible substrate, and [16], in which the layout of the antenna and the rectifier is embroidered with conductive thread on a felt fabric, the radiating elements are manufactured by stacking conductive and dielectric felt fabric sheets. Regarding the rectifier, in all the considered rectennas, with the exception of [16], in which the rectifier components are soldered to the textile paths, the circuits are implemented in conventional PCB substrates and then soldered to the antenna terminals, providing a poor degree of integration and robustness. Therefore, the obtained results show that the presented rectenna provides an electrical performance comparable to the state-of-the-art for textile devices, whereas the use of fully-woven technology and the proposed rectifier integration technique contribute to improve the integration level and the robustness with respect to other textile technologies.

VI. CONCLUSION

A circularly polarized fully woven textile rectenna for Wireless Power Transfer applications in the 2.4 GHz band was presented. The radiating element is fed through a T-match

network which enables complex conjugate impedance matching with the rectifier circuit without requiring any additional impedance matching network or elements. The rectifier circuit is based on a single Schottky diode, and it was optimized for a −10 dBm input power level, which is a realistic value when taking into account the European EIRP limit for indoor applications in the considered band. The circuit is mounted on a carrier thread and then introduced into the woven structure. This implementation approach, combined with the radiating element feeding technique, provides a high degree of integration between the rectifier and the woven antenna. The rectenna was experimentally characterized, obtaining an overall 45% RF-DC conversion efficiency when the available power at the rectifier input is −10 dBm. It was also evaluated for higher input power values, showing that the conversion efficiency improves with the available power. Hence, the presented rectenna can provide better performance in regions with higher EIRP limits, or when reducing the distance between transmitter and receiver. The obtained efficiency is close to the simulated value, validating the design and implementation processes. Furthermore, it is comparable to the state-of-the-art values for textile nonwoven rectennas, whereas the use of fully-woven technology and the proposed integration technique contribute to improving the robustness and the degree of integration. To the best of the author's knowledge, this is the first reported fully woven textile rectenna in which the rectifier is integrated into the woven structure.

REFERENCES

[1] M. Wagih, "Microwave-enabled wearables: Underpinning technologies, integration platforms, and next-generation roadmap," *IEEE J. Microw.*, vol. 3, no. 1, pp. 193–226, Jan. 2023, doi: 10.1109/JMW.2022.3223254.

[2] S. Kim, R. Vyas, J. Bito, K. Niotaki, A. Collado, A. Georgiadis, and M. M. Tentzeris, "Ambient RF energy-harvesting technologies for self-sustainable standalone wireless sensor platforms," *Proc. IEEE*, vol. 102, no. 11, pp. 1649–1666, Nov. 2014, doi: 10.1109/JPROC.2014.2357031.

[3] M. Piñuela, P. D. Mitcheson, and S. Lucyszyn, "Ambient RF energy harvesting in urban and semi-urban environments," *IEEE Trans. Microw. Theory Techn.*, vol. 61, no. 7, pp. 2715–2726, Jul. 2013, doi: 10.1109/TMTT.2013.2262687.

[4] S. Saab, N. Kouzayha, A. Eid, A. A. Benbuk, J. Costantine, and Z. Dawy, "Recycling ambient Wi-Fi signals for low energy wake-up of wireless sensors," *IEEE Sensors Lett.*, vol. 4, no. 10, pp. 1–4, Oct. 2020, doi: 10.1109/LSENS.2020.3026236.

[5] A. J. Williams, M. F. Torquato, I. M. Cameron, A. A. Fahmy, and J. Sienz, "Survey of energy harvesting technologies for wireless sensor networks," *IEEE Access*, vol. 9, pp. 77493–77510, 2021, doi: 10.1109/ACCESS.2021.3083697.

[6] M. Wagih, A. S. Weddell, and S. Beeby, "Rectennas for radio-frequency energy harvesting and wireless power transfer: A review of antenna design [antenna applications corner]," *IEEE Antennas Propag. Mag.*, vol. 62, no. 5, pp. 95–107, Oct. 2020, doi: 10.1109/MAP.2020.3012872.

[7] Y.-S. Chen and C.-W. Chiu, "Maximum achievable power conversion efficiency obtained through an optimized rectenna structure for RF energy harvesting," *IEEE Trans. Antennas Propag.*, vol. 65, no. 5, pp. 2305–2317, May 2017, doi: 10.1109/TAP.2017.2682228.

[8] U. Olgun, C.-C. Chen, and J. L. Volakis, "Investigation of rectenna array configurations for enhanced RF power harvesting," *IEEE Antennas Wireless Propag. Lett.*, vol. 10, pp. 262–265, 2011, doi: 10.1109/LAWP.2011.2136371.

[9] M. Wagih, N. Hillier, S. Yong, A. S. Weddell, and S. Beeby, "RF-powered wearable energy harvesting and storage module based on E-textile coplanar waveguide rectenna and supercapacitor," *IEEE Open J. Antennas Propag.*, vol. 2, pp. 302–314, 2021, doi: 10.1109/OJAP.2021.3059501.

[10] M. Wagih, A. S. Weddell, and S. Beeby, "Omnidirectional dual-polarized low-profile textile rectenna with over 50% efficiency for sub-μW/cm^2 wearable power harvesting," *IEEE Trans. Antennas Propag.*, vol. 69, no. 5, pp. 2522–2536, May 2021, doi: 10.1109/TAP.2020.3030992.

[11] S.-E. Adami, P. Proynov, G. S. Hilton, G. Yang, C. Zhang, D. Zhu, Y. Li, S. P. Beeby, I. J. Craddock, and B. H. Stark, "A flexible 2.45-GHz power harvesting wristband with net system output from -24.3 dBm of RF power," *IEEE Trans. Microw. Theory Techn.*, vol. 66, no. 1, pp. 380–395, Jan. 2018, doi: 10.1109/TMTT.2017.2700299.

[12] M. Wagih, G. S. Hilton, A. S. Weddell, and S. Beeby, "Dual-band dual-mode textile antenna/rectenna for simultaneous wireless information and power transfer (SWIPT)," *IEEE Trans. Antennas Propag.*, vol. 69, no. 10, pp. 6322–6332, Oct. 2021, doi: 10.1109/TAP.2021.3070230.

[13] M. Wagih, G. S. Hilton, A. S. Weddell, and S. Beeby, "Broadband millimeter-wave textile-based flexible rectenna for wearable energy harvesting," *IEEE Trans. Microw. Theory Techn.*, vol. 68, no. 11, pp. 4960–4972, Nov. 2020, doi: 10.1109/TMTT.2020.3018735.

[14] Z. Chen, C. Song, J. Zhang, X. Zheng, V. Volskiy, P. Chu, and G. A. E. Vandenbosch, "Wearable rectenna with integrated miniaturized feeding slot and rectifier structure," *IEEE Trans. Antennas Propag.*, vol. 71, no. 5, pp. 3868–3881, May 2023, doi: 10.1109/TAP.2023.3249827.

[15] C.-X. Mao, D. Vital, D. H. Werner, Y. Wu, and S. Bhardwaj, "Dual-polarized embroidered textile armband antenna array with omnidirectional radiation for on-/off-body wearable applications," *IEEE Trans. Antennas Propag.*, vol. 68, no. 4, pp. 2575–2584, Apr. 2020, doi: 10.1109/TAP.2019.2951517.

[16] D. Vital, S. Bhardwaj, and J. L. Volakis, "Textile-based large area RF-power harvesting system for wearable applications," *IEEE Trans. Antennas Propag.*, vol. 68, no. 3, pp. 2323–2331, Mar. 2020, doi: 10.1109/TAP.2019.2948521.

[17] J. Antonio Estrada, E. Kwiatkowski, A. López-Yela, M. Borgoñós-García, D. Segovia-Vargas, T. Barton, and Z. Popovic, "RF-harvesting tightly coupled rectenna array tee-shirt with greater than octave bandwidth," *IEEE Trans. Microw. Theory Techn.*, vol. 68, no. 9, pp. 3908–3919, Sep. 2020, doi: 10.1109/TMTT.2020.2988688.

[18] L. Alonso-Gonzalez, S. Ver-Hoeye, M. Fernandez-Garcia, and F. Las Heras Andres, "Three-dimensional fully interlaced woven microstrip-fed substrate integrated waveguide," *Prog. Electromagn. Res.*, vol. 163, pp. 25–38, 2018, doi: 10.2528/pier18040207.

[19] L. Alonso-González, S. Ver-Hoeye, M. Fernández-García, and F. Las-Heras Andrés, "Broadband flexible fully textile-integrated bandstop frequency selective surface," *IEEE Trans. Antennas Propag.*, vol. 66, no. 10, pp. 5291–5299, Oct. 2018, doi: 10.1109/TAP.2018.2858141.

[20] L. Alonso-Gonzalez, S. Ver-Hoeye, M. Fernandez-Garcia, and F. Las Heras Andres, "Layer-to-layer angle interlock 3D woven bandstop frequency selective surface," *Prog. Electromagn. Res.*, vol. 162, pp. 81–94, 2018, doi: 10.2528/pier18041707.

[21] L. Alonso-González, S. Ver-Hoeye, M. Fernández-García, Y. Álvarez-López, C. Vázquez-Antuña, and F. L. Andrés, "Fully textile-integrated microstrip-fed slot antenna for dedicated short-range communications," *IEEE Trans. Antennas Propag.*, vol. 66, no. 5, pp. 2262–2270, May 2018, doi: 10.1109/TAP.2018.2814203.

[22] L. Alonso-Gonzalez, S. Ver-Hoeye, M. Fernandez-Garcia, C. Vazquez-Antuna, and F. Las-Heras Andres, "On the development of a novel mixed embroidered-woven slot antenna for wireless applications," *IEEE Access*, vol. 7, pp. 9476–9489, 2019, doi: 10.1109/ACCESS.2019.2891208.

[23] L. Alonso-Gonzalez, S. Ver-Hoeye, C. Vazquez-Antuna, M. Fernandez-Garcia, and F. Las-Heras Andres, "Multifunctional fully textile-integrated RFID tag to revolutionize the Internet of Things in clothing [wireless corner]," *IEEE Antennas Propag. Mag.*, vol. 61, no. 3, pp. 104–110, Jun. 2019, doi: 10.1109/MAP.2019.2907910.

[24] S. V. Hoeye, M. Fernández, L. Alonso, C. V. Antuña, P. Ghekiere, and J. A. Casas, "A novel surface-independent textile fully woven UHF RFID tag," *IEEE Trans. Antennas Propag.*, vol. 70, no. 11, pp. 10156–10165, Nov. 2022, doi: 10.1109/TAP.2022.3191159.

[25] G. Marrocco, "The art of UHF RFID antenna design: Impedance-matching and size-reduction techniques," *IEEE Antennas Propag. Mag.*, vol. 50, no. 1, pp. 66–79, Feb. 2008, doi: 10.1109/MAP.2008.4494504.

[26] L. Alonso-González, S. Ver-Hoeye, M. Fernández-García, C. Vázquez-Antuña, and F. Las-Heras Andrés, "From threads to smart textile: Parametric characterization and electromagnetic analysis of woven structures," *IEEE Access*, vol. 7, pp. 1486–1501, 2019, doi: 10.1109/ACCESS.2018.2886041.
[27] L. Alonso-González, S. Ver-Hoeye, C. Vázquez-Antuña, M. Fernández-García, and F. Las-Heras Andrés, "On the techniques to develop millimeter-wave textile integrated waveguides using rigid warp threads," *IEEE Trans. Microw. Theory Techn.*, vol. 66, no. 2, pp. 751–761, Feb. 2018, doi: 10.1109/TMTT.2017.2777983.

MIGUEL FERNÁNDEZ received the M.Sc. degree in telecommunication engineering, the M.Sc. degree in information technology and mobile communications, and the Ph.D. degree from the University of Oviedo, Gijón, Spain, in 2006, 2010, and 2010, respectively.

From 2006 to 2008, he was a Research Fellow with the Signal Theory and Communications Group, University of Oviedo. Since September 2008, he has been an Associate Professor with the Signal Theory and Communications Group, University of Oviedo. His main research interests include nonlinear analysis and optimization techniques for the design of oscillator-based circuits, active antennas, and frequency multipliers and mixers at the microwave, millimeter/submillimeter-wave, and terahertz frequency bands.

CARLOS VÁZQUEZ received the M.Sc. degree in telecommunication engineering, the M.Sc. degree in information technology and mobile communications, and the Ph.D. degree from the University of Oviedo, Gijón, Spain, in 2007, 2008, and 2013, respectively.

From 2007 to 2012, he was a Graduate Research Assistant, from 2012 to 2021, he held different research and technical positions, and since 2021, he has been an Assistant Professor with the Signal Theory and Communications Group, University of Oviedo. His research efforts have extended across different fields, including the nonlinear analysis and optimization techniques for the design of multifunctional oscillator-based circuits, antennas, and passive components, such as frequency multipliers and harmonic mixers, at microwave, millimeter/submillimeter-wave, and terahertz frequencies. In the last few years, he has been focused on the design of fully textile-integrated circuits and antennas, suitable for mass production using common processes in the textile industry.

SAMUEL VER HOEYE (Member, IEEE) received the M.Sc. degree in electronics engineering from the University of Ghent, Ghent, Belgium, in 1999, and the Ph.D. degree from the University of Cantabria, Santander, Spain, in 2002.

He is currently a Full Professor with the Department of Electrical and Electronic Engineering, University of Oviedo, Gijón, Spain. His main research interests include the design and analysis of microwave, millimeter wave, and THz circuits and systems. Among these are the multi-functional oscillator-based circuits and antennas, frequency scanning antennas, graphene-based frequency multipliers and mixers, imaging systems, and textile-integrated high-frequency components.